Ion release characterization in phase separated borosilicate glass powders

Federico Lizzi, Christelle Goutaudier, Nina Attik, Philip Jackson, Ian Campbell, Ilham Mokbel, Brigitte Grosgogeat, Cyril Villat

Ion release characterization in phase separated borosilicate glass powders

Federico Lizzi[1,2], Christelle Goutaudier[1], Nina Attik[1,4], Philip Jackson[2], Ian Campbell[2], Ilham Mokbel[1], Brigitte Grosgogeat[1,3,4], Cyril Villat*[1,3,4]

1 Laboratoire des Multimatériaux et Interfaces,UMR CNRS 5615, Univ Lyon, Université Claude Bernard Lyon 1, CNRS, F-69622 Villeurbanne, France

2 Lucideon Inc., Penkhull, Stoke-On-Trent ST4 7LQ, UK

3 Service d'odontologie, Hospice Civils de Lyon, Lyon, France

4 Faculté d'Odontologie, Université Claude Bernard Lyon 1, Lyon, France

1. Introduction

In 1969, Hench developed the first bioglass containing Na_2O; CaO; SiO_2 and P_2O_5. Since then, the initial Hench Bioglass® has been widely studied and modified to improve its biological, antibacterial and mechanical properties. Moreover, bioglasses may exhibit phase separation that could have an impact on their biological properties. The particular structure and the properties deriving therefrom depend on their thermal history as well as their preparation technique and their composition. [1-8]

Among the different bioglasses investigated during these past five decades, borosilicate glasses have shown interesting bioactive properties in bone repair and in drug delivery systems [4]. These glasses are also well known to exhibit phase separation. The earliest practical application of phase separation has been developed by Hood and Nordberg [9] in the Vycor process (SiO_2, B_2O_3, Na_2O glass system) for the production of high silica ware via a porous glass approach.

The amorphous phase separation (APS) causes an initially homogeneous single phase glass to separate into two or more phases of different compositions. The Gibbs free energy of the system with two or more distinct phases has to be lower than that of the system with one single homogeneous phase. The degree of interconnectivity of the two glass phases depends on the nature of the phase separation mechanism. This process can occur by a nucleation and growth process (which gives isolated spherical particles) or by spinodal decomposition where an interconnected structure is obtained [10].

Considering the borosilicate glass composition, boron impacts on the release into aqueous media of other elements such as calcium and, hence, on the bone metabolism. Boron has been linked with preventing calcium loss and bone demineralization in post-menopausal women

and boron supplementation has been shown to reduce the effects of vitamin D deficiency in chicks. It also clearly influences bone-regulating hormones involved in bone growth and bone turnover. In terms of other elements used in silicate glasses, calcium is useful since it is a primary component of hydroxyapatite in bone but also in dental tissues (enamel and dentin) and so, is crucial for the restoration of damaged hard tissue. Potassium is a useful desensitizing agent. Aluminium has been considered as an important element for providing Al^{3+} ions that are useful for the secondary self-hardening process in dental cements featuring polyacids. Nonetheless, Aluminium is recognized as a neurotoxin and the cause of some neurological diseases, such Alzheimer's and Parkinson's disease [11-16].

Considering the properties described above, phase-separated glass systems composed of SiO_2-K_2O-B_2O_3-CaO-Al_2O_3 could be of interest in medicine and dentistry due to their ion release potential and post-leaching increased porosity. However, the behaviour of such materials should be investigated in acidic conditions to evaluate their possible uses blended with polyacid solutions or in the oral environment where pH changes due to food consumption are experienced. In the work reported here, different compositions have been investigated in which SiO_2 and K_2O were fixed (45% and 15% in weight respectively) while other elements (Ca, Al, B) varied in order to assess the effect on phase separation. In the perspective of biomedical and dental use i.e. in glass ionomer cements (GIC), this study investigates the acid degradability and leaching profile of the ions released from novel borosilicate fillers into a nitric acid solution at different time points. The different composition of borosilicate samples have been obtained with a factorial experimental design (FED) that allows the efficient organization of the experiments required in scientific research or industrial process optimisation. The hypothesis is that the phase separation would directly influence the ion release behaviour and subsequently the poly-acid cement setting. Structural properties of the glasses, physico-chemical and morphological features related to the phase separation and ion release are investigated in this study and correlated to the glass composition.

2. Material and methods

2.1. Borosilicate glass preparation

Using a Factorial Experimental Design (FED) approach, a series of glass compositions based on the quinary system SiO_2-B_2O_3-K_2O-Al_2O_3-CaO (Table1) were prepared from raw materials purchased by different manufacturers:

- Microsil (Sibelco Benelux, Antwerpen, Belgium) 99% pure SiO_2,
- H_3BO_3 (Optibor TP, Borax Inc, Rio Tinto Borates, Greenwood Village, CO, USA),
- K_2CO_3 (Altair Chimica SpA, Saline di Volterra, Italy),
- $Al_2(OH)_6$ (Industrial Mineral Services, Madeley, United Kingdom) and,
-$CaCO_3$ (Ben Bennett Jr Ltd, Rotherham, United Kingdom).

As mentioned above, SiO_2 and K_2O were fixed at, respectively, 45% and 15% by weight in the developed glasses. The phase-separated borosilicate (PSBS) glasses were synthesized using the melt-quenching technique. The batch was melted at 1200-1300 °C (the temperature selected for each composition being based on visual assessment during melting) in a quartz crucible for 4 hours in an electrically heated furnace. The melt was quenched by pouring onto a flat steel plate. The resulting glasses were then heat treated at 700°C for 20 hours to induce phase-separation. Two duplicate batches (PSBS 7 and PSBS 10; PSBS2 and PSBS 6) were made in order to compare the results obtained after melting to avoid possible experimental errors. Finally, a fraction of each sample was milled with a Tema mill (Tema Machinery Ltd, Woodford Halse, United Kingdom) to obtain a particle size of about 50µm.

2.2 Characterization of the borosilicate glasses

2.2.1. X-ray powders diffraction

Powder X-ray diffraction (XRD) data were collected with a Bruker diffractometer with graphite monochromator (Bruker Ltd, Coventry, United Kingdom) using CuKα radiation. Data were collected in the range of $2° < 2\theta < 60°$ in 0.05° steps.

This technique was used to determine if the glass frit was fully amorphous after the heat treatment.

2.2.2 Particle size distribution analysis

The particle size distribution was measured by the Malvern Mastersizer 3000 laser diffraction particle size analyser (Malvern Panalytical Ltd, Malvern, United Kingdom). The glass powders were evaluated in liquid dispersion with ethanol to avoid unwanted aqueous dissolution and to ensure a consistent Dv99 of less than 50 µm and a Dv50 of less than 6.9

µm. Three collections of powders measurements were made for waiting the stabilization of the dispersion.

2.2.3. Differential thermal analysis

Thermal behaviour was analysed using differential thermal analysis (DTA) on a TGA/DSC 2 apparatus (Mettler Toledo, Viroflay, France). The measurements were conducted with a heating rate of 20°C/min and using nitrogen as both a protecting and a purge gas. Approximately 50 mg of glass powder was placed into an alumina crucible and gently pressed to ensure good heat transfer. The powders were scanned over the 30 to 1200°C range. The calibration of the DSC equipment in terms of temperature was done by using the theoretical values of four metal standards for which the precise values of melting temperatures are well known (In; Al; Au and Pd). The relative uncertainty does not exceed 0.3% for temperature. The glass transition temperature was measured at the inflection point of the sigmoid characterizing it.

2.2.4. Static dissolution experiments

Static dissolution experiments were performed for all the PSBS samples. The glass powders (0.4 g each) were mixed with an HNO_3 0.003M aqueous solution (40.0 mL) in a flacon tube. The mixtures were stirred in a 37°C thermostatically controlled reactor. The pH of the mixture was recorded during the entire dissolution process. The absolute uncertainty of the pH values is u(pH) = 0.02 after calibration of the meter with pH 4; 7 and 10 buffers. At different time points, the solutions were centrifuged and collected to quantify the ions released.

2.2.5. Inductively coupled plasma atomic emission spectroscopy

The amount of ions released in the collected solutions was measured by inductively coupled plasma atomic emission spectroscopy (Vista-MPX CCD Simultaneous ICP-OES, Varian Inc., Palo Alto, USA). The elements detected and the corresponding absorption wavelengths are reported in table 2. Calibration curves were obtained by preparing multi-elements standard solutions containing B, Ca, K and Si (dilutions were made in HNO_3 solutions). Aluminium

was not detected with the ICP measurements for all the glasses because it is highly insoluble in aqueous solution from pH=2 to 10. Due to its amphoteric nature, Al_2O_3 can react with both bases and acid. According to the pH of the medium, it precipitates as aluminium hydroxide or alkaline aluminate as it is released in the solution. Three replicates were collected for each measurement. The concentration values obtained from different emission lines for each element were averaged and presented as percentage of dissolved element ([element]%), calculated as the ratio between the measured concentration and the maximum concentration that could be obtained if total dissolution of the glass occurred. The main source of uncertainty is due to the scattering of the experimental points emerging from analysis procedure. The relative standard uncertainty u_r([element]%) is estimated as twice the value of the variation coefficient of the 3 replicates.

Consequently, the mean values of u_r are as follow: u_r([element]%) = 3% for Boron, Calcium and Silicon, and u_r([element]%) = 5% for Potassium. These values are in good agreement with those commonly accepted for ICP technique.

2.2.6. Scanning electron microscopy (SEM)

Glass bulk specimens were mounted in a methyl methacrylate resin (Resine mecaprex KM-U, Prési, Brié-et-Angonnes, France) then polished by a NWF+ (Rough-finishing cloths, Prési, Brié-et-Angonnes, France) with a 3µm diamond suspension, in order to obtain a flat surface. The morphology of the samples was examined using a scanning electron microscope incorporating EDX analysis (FEI Quanta FEG 250, Thermo Fisher Scientific, Villebon-sur-Yvette, France) before and after two acid treatments. The leaching of bulk glasses was performed using (i) ambient conditions comprising a 1 M HNO_3 etch at 37°C for 48 hours and (ii) “hard” conditions (as (i) but at 90°C). Then, the glasses were rinsed with deionized water before analysis. The hard condition was carried out to speed up the dissolution process to more completely etch out the most soluble phase (postulated to be the boron-rich one) from the samples.

2.2.7 X-ray fluorescent analysis (XRF)

XRF analysis was used to analyse the oxide type and content in the glass powder obtained after the dissolution experiments featuring the hard condition. The material was ground to a

powder and ignited to attain a constant weight; the ignited material was mixed with a flux and a glass melt formed. The melt was casted into a bead and run on the Panalytical Axios WD XRF spectrometer (Malvern Panalytical Ltd, Malvern, United Kingdom). A bulk chemical analysis has then obtained.

3. Results

3.1.Glasses characterization

All the PSBS glasses were amorphous according to the XRD results before and after the heat-treatment. However, whilst the as-quenched samples appeared consistently transparent and colourless, the thermal treatment at 700°C for 20 hours induced some of the samples to turn opalescent. The intensity of this phenomenon varies from a slight milky effect until completely opaque. The diagram in figure 1 shows that the composition influences the opacity of the samples and suggests lines (isopleths) associated with intense, mild or no opacification. In the absence of crystalline phases, the opacification is most likely linked to a phase separation leading to two glass phases with different refractive index (RI).

With the SiO_2 and K_2O content being fixed, Janecke's coordinates (w_i^J) were employed to enable glass compositions to be plotted on a triaxial diagram. This allows better visualisation of the impact of varying Al_2O_3, CaO and B_2O_3 content (fig.1):

$w_i^J = \frac{m_i}{\sum_i m_i}$ where m_i represents the mass of each component Al_2O_3, CaO and B_2O_3

Powder X-ray diffraction (XRD) analysis was performed for every sample after the heat treatment. All the XRD spectra patterns show a characteristic amorphous shape and do not demonstrate the formation of a secondary amorphous phase. Figure 2 shows some typical XRD results of glasses without Al_2O_3 (Figure 2a) and without CaO (figure 2b).

For samples without Al_2O_3, the superposition of the resulting patterns shows a 2θ angle shift of the typical amorphous halo. It has been found to be related to the level of CaO addition in the sample compositions (Table 3).

DTA analyses were carried out on four carefully chosen samples to evaluate the influence of composition on the glass structure. Thermograms for PSBS 1, 3, 4 and SBK are showing a

principal glass transition Tg, corresponding to the major amorphous phase (Figure 3). Other less pronounced shifts in the DTA curves are evidence of the presence of a second phase, probably corresponding to the other phase formed after the heat treatment. The Tg is influenced by the introduction of alkaline earth oxides and aluminium addition (Table 4), considering that the w% potassium is the same for all samples. Ca^{2+} causes an increase in the Tg temperature in respect to the three component glass PSBS SBK. However, the order of Tg increase does not correlate to calcium loading suggesting that aluminium also plays a significant role in creating increased glass network connectivity and so a higher Tg. The presence of phase separation serves to further complicate the situation.

3.1.1 Observation of the PSBS3 at T above the T_g

Only one sample, the most calcium-rich sample PSBS 3, presents an exothermic peak at 787.8°C in the DTA curve. This heat production phenomenon demonstrated by a rapid change in the heat flow, appears when a glass arranges into a more ordered structure characteristic of crystals. This crystallisation temperature (Tc) converts the glass into a glass-ceramic.

The crystallization process has been amplified by a heat treatment at different time-points (5, 10 and 20 hours) and at a temperature (800°C) higher than the phase separation heat treatment. Pictures of the resulting sectioned samples were taken with the optical microscope and show the development of the crystallisation process from the external surface to the core of the bulk sample (Fig. 4).

The crystalline phases are revealed by XRD analysis (Fig. 5) and identified as:

- Potassium Boro-Silicate ($KBSi_2O_6$),
- Calcium Borate (CaB_2O_4),
- Tri-Calcium Silicate (Ca_3SiO_5).

3.2.Static dissolution experiments

In a first step, the PSBS powder samples have been compared by measuring the pH variation in HNO_3 (0.003M aqueous solution). All glasses show the same characteristic pH curve typical of bioactive glasses when dispersed in aqueous media (Fig. 6). A rapid pH increase takes place during the first minutes, after which the pH increases only slightly. This

phenomenon is due to the ionic exchange between the cationic network modifiers and H^+ in the HNO_3 solution. After the fast pH rise, stabilization at between pH 8 and 9 occurs. The pH rise is considerably accelerated by the heat-treatment suggesting a low chemical durability phase with a higher concentration of potassium.

Hydrolysis of the silica network is known to occur at higher pH values (usually above pH=10), resulting in congruent dissolution of silicate glasses [17]. Consequently, this phenomenon must be negligible in the conditions used.

The comparison of samples with and without Al_2O_3 reveals a different ion leaching behaviour during time (Fig. 7). PSBS 16 (opalescent glass, 15 w% of Al_2O_3) releases calcium at a higher kinetic rate ($\Delta Ca/\Delta t$ = 2.98 Ca%/min). For PSBS8 (transparent glass, without Al_2O_3), the release of potassium and boron is congruent and happens at a faster kinetic rate than calcium ($\Delta K/\Delta t$ = 2.74 K%/min; $\Delta B/\Delta t$ = 2.66 B%/min). Silicon release is very low for both the glass samples. This is to be expected as it is a network former and not prone to leaching. It is also likely that silicon is dominant in the more durable of the two phases. Boron and potassium are released much more readily than silicon. Fast potassium release is to be expected but boron, like silicon, might be expected to play a network former role in the generation of stable glasses. However, glasses with a high Boron content can have lower durability and in this case, the release can be similar to a network modifier ion such as K^+. The formation of NBO (non-bridging oxygens) weakens the structure of glass and makes the species soluble and more accessible to water. The depolymerisation of the silica network by the creation of NBO generates larger cavities, favouring the invasion of nitric acid solution and the exit of the soluble elements. Two mechanisms of dissolution are hypothesized for PSBS8 and PSBS16; after 125 minutes in HNO_3, a rapid increase in ion release is detected in PSBS8. The phenomenon is not detected in PSBS16 where after 125 minutes it appears that the ion release reaches a plateau. PSMS8 is postulated to have a weaker glass phase (featuring potassium and boron at high levels) that more readily dissolves. In addition, the faster release of calcium from the opalescent glass could bring about the formation of a precipitate layer on the glass surface that delays further release of other species resulting in a plateau. The release of aluminium ions is not reported because detection is at too low concentrations. This suggests Al ends up in the resistant phase and could encourage the progress of phase separation during the heat-treatment promoting the formation of opalescent glasses.

A comparison between two samples PSBS3 and PSBS5 (transparent and opalescent respectively, with the same amount of calcium in the compositions) has been made in figure

8. The ion concentration profiles suggest that the dissolution rate of Ca and B are enhanced by the heat treatment in all cases. Moreover, it is confirmed that different leaching rates exist between the opal and clear samples. In PSBS3 potassium ions are released with a higher kinetic rate than PSBS5 ($\Delta K/\Delta t$ = 9.5E-3 vs. 5.3E-3), while for calcium ions the opposite tendency is observed ($\Delta Ca/\Delta t$ = 8E-3 vs. 11.2E-3).

In figure 9 are shown the boron, calcium, potassium and silicon release trends for glasses belonging to specific isopleths for the two main glass series (transparent and opalescent) identified in figure 1. The isopleths identify compositions with a constant amount of aluminium. The ion release profiles confirm that the opalescent glasses release calcium with a faster kinetic rate than the transparent ones (average comparison of the kinetic rate is 4 and 2.65 $\Delta Ca/\Delta t$ respectively). Potassium is released faster in the transparent samples (average rate: 3.18 $\Delta K/\Delta t$) compared to the opalescent ones (average kinetic rate: 2.38 $\Delta K/\Delta t$). The dissolution mechanism for both glass series is found to be dependent from the B_2O_3/CaO ratio. This value has been represented in the graphs using the Janecke's coordinates without taking in consideration the amount of Al_2O_3 because it is assumed to be constant along the isopleths. Higher amounts of boron in the composition induce a slower release of potassium, calcium and boron which is justified by a higher borosilicate character in the weaker phase of the glasses.

3.3 Scanning electron microscopy

SEM analyses of the PSBS 8 and PSBS 16 glass bulk samples were undertaken to find evidence for two amorphous phases and to confirm that phase separation was occurring. It was expected to find similarity with the sodium borosilicate system of the Vycor glasses. Figure 10 represents the analysis of the glass surface with the back-scatter detector and shows two different structures for the opalescent and the transparent surfaces. The left-hand images (opalescent sample) present a number of sparse droplets ranging in size between 20 and 30 nm whilst the right-hand images suggest narrow veins surrounded by a homogeneous phase.

The etching process in normal conditions is found to be effective for revealing new details of the glass surface. A porous structure is detected for the opalescent sample PSBS 16 while a homogeneous surface without narrow veins is observed in the transparent glass PSBS 8 (see lower images in figure 10), proving that the surfaces are different and a distinct reaction with the nitric acid is going on. In order to increase the dissolution phenomenon, the glasses were

immersed in nitric acid in hard conditions (temperature = 90°C). This hard acidic condition reveals more details for the interpretation of the glass structures:

- The opalescent bulk glass (PSBS 16) shows a high level of structure retention with the leach surface again showing porosity. EDX analysis identified pure silica (Fig. 11),

- The transparent bulk glass (PSBS 8) has dissolved significantly, leading to structure collapse and leaving, at the bottom of the reaction beaker, a white amorphous powder composed of almost pure silica as shown by XRD and XRF analyses (Fig. 12).

4. Discussion

The present study illustrated the properties of borosilicate glasses in relation to their thermal history and contrasts ion leaching behaviour before and after heat treatment of a range of compositions. The selected compositions simulated the SiO_2 content of 45S5 glass [18] and using K_2O as alkali selected a compositional range based on reported development of phase separated structure [19]. In addition to compositional factors affecting the parent glass properties, thermal treatment was shown to consistently alter phase structures, depending on composition, and therefore properties as shown by relative pH changes vs time (figure 6) and relative leaching (figures 8 and 9) [20].

Two obvious glass types were apparent after heat treatment observed as transparent and opalescent products. Results indicated that opalescence must be the result of glass in glass phase separation, as crystallisation was typically not encountered with the selected heat treatment regime. Although difficult to see in figure 3, second Tg values were apparent even for transparent glasses. Only at high calcium levels and/or higher heat treatment temperatures was a crystallisation event seen (figure 3). Transparency in phase-separated glasses can either be a result of forming two phases with the same refractive index or the presence of one phase as nano-size entities [21].

Dissolution behaviour was considered typical of bioactive glasses in aqueous media [1, 22]. However, the influence of heat treatment on individual cases must always be considered in connection with compositional factors. Heat treatment creating both opalescent and transparent phase-separated glasses leads to a change in ion dissolution behaviour (figure 8). Thereby, a chemically weaker phase and a chemically stronger phase are created [23] in both

cases but much more work is needed to identify the composition and size / availability of the weaker phase in both cases.

Microscopy (figure 10) showed some evidence of phase separated structures with differences evident in between opalescent and transparent phase separated glasses. Opalescent glasses show clear evidence of smaller, discrete areas of weak glass becoming leached out. Microscopic analysis for the transparent glass is less clear: A vein-like structure before leaching vanishes after leaching. The fact the transparent samples collapse to a powder after "hard" acid leaching suggests a weaker continuous glass layer with discrete, perhaps nano-size regions of a high silica durable phase that ultimately becomes powder (figure 13).

The final structures and compositions of the individual amorphous phases dictate the leaching of elements and the nature of any relict structure or material. It is doubtful whether SEM-EDX can provide compositional information on each phase. Techniques such as Helium Ion Beam Microscopy may be needed. Alternatively, more work could be performed on analysis on the remaining phase (assuming 100% leaching of the weak phase can be guaranteed) to provide, by difference, the composition of the leached phase. It would be interesting to compare the calculated leached phase to the ppm levels of ions leached from the phase versus time. Whilst it is clear that calcium and aluminium ions play a significant role in creating glass structure connectivity and so degree of leaching in acids, until the relative level of calcium, aluminium and boron in the weakest phase is known, it is difficult to connect structure to leaching trends [24]. Of particular interest in the field of GICs is the performance / behaviour of transparent phase-separated glasses that contain no aluminium. Although not reported here, very preliminary data suggests a powdered version of the transparent glass delivers an impressive set strength. In the absence of alumina, it is postulated that leaching of boron (as borates) creates cross-linking opportunities.

In summary, the present study suggests a free alumina borosilicate glass with an enhanced bioactivity and apatite forming ability. Despite the need for much more work, it is clear that the ability to influence the dissolution behaviour of these glasses indicates potential development for improved biomedical materials such as glass ionomer cement in restorative dentistry, in particular. Formulation of Al free varieties of dental cements has already been proposed in previous studies with different approaches [25-27].

Conflicts of interest

The authors declare no conflicts of interests.

Acknowledgements

The research leading to this research article has received funding from the European Union Seventh Framework Program (FP7/2007-2013) under grant agreement n◦608197.

References

[1] J.R. Jones, Review of bioactive glass: From Hench to hybrids, Acta Biomater, 9 (2013) 4457-4486.

[2] W. Li, H. Wang, Y. Ding, E.C. Scheithauer, O. Goudouri, A. Grünewald, R. Detsch, S. Agarwal, A.R. Boccaccini, Antibacterial 45S5 Bioglass®-based scaffolds reinforced with genipin cross-linked gelatin for bone tissue engineering, J. Mater. Chem. B 3 (2015) 3367-3378.

[3] F. Lizzi, C. Villat, N. Attik, P. Jackson, B. Grosgogeat, C. Goutaudier, Mechanical characteristic and biological behaviour of implanted and restorative bioglasses used in medicine and dentistry: A systematic review, Dent. Mater. 33 (2017) 702-712.

[4] E. Fiume, J. Barberi, E. Verné, F. Baino, Bioactive Glasses: From Parent 45S5 Composition to Scaffold-Assisted Tissue-Healing Therapies, J. Funct. Biomater. 9 (2018) 24.

[5] L. Lefebvre, L. Gremillard, J. Chevalier, R. Zenati, D. Bernache-Assolant, Sintering behaviour of 45S5 bioactive glass, Acta Biomater. 4 (2008) 1894-1903.

[6] R. Golovchak, P. Thapar, A. Ingram, D. Savytskii, H. Jain, Influence of phase separation on the devitrification of 45S5 bioglas,. Acta Biomater. 10 (2014) 4878-4886.

[7] D. Durgalakshmi, S. Balakumar, Phase separation induced shell thickness variations in electrospun hollow Bioglass 45S5 fiber mats for drug delivery applications, Phys. Chem. Chem. Phys. 17 (2015) 15316-15323.

[8] H. Liu, R.E. Youngman, S. Kapoor, L.R. Jensen, M.M. Smedskjaerb, Y. Yue, Nano-phase separation and structural ordering in silica-rich mixed network former glasses, Phys. Chem. Chem. Phys. 20 (2018) 15707-15717.

[9] P.F. James, Volume Nucleation in Silicate Glasses, in: M.H. Lewis (Ed), Glasses and glass ceramics, Springer Netherlands, 1989, pp 59-105.

[10] D.R. Uhlmann, Microstructure of glasses does it really matter, J. Non-Crystal. Sol. 49 (1982) 439-460.

[11] M.R. Naghii, S. Samman, The role of boron in nutrition and metabolism, Progress Food Nutri. Sci. 17 (1993) 331-349.

[12] N. King, T.W. Odom, H.W. Sampson, A.G. Yersin, The Effect of In Ovo Boron Supplementation on Bone Mineralization of the Vitamin D-Deficient Chicken Embryo, Biol. Trace Elem. Res. 31 (1991) 223-233.

[13] C. Palacios, The Role of Nutrients in Bone Health, from A to Z, Crit. Rev. Food Sci. Nutr. 46 (2006) 621-628.

[14] B.A. Matis, M.A. Cochran, G.J. Eckert, J.I. Matis, In Vivo Study of Two Carbamide Peroxide Gels with Different Desensitizing Agents, Oper. Dent. 32 (2007) 549-545.
[15] J.W. Nicholson, B. Czarnecka, Role of Aluminum in Glass-ionomer Dental Cements and its Biological Effects, J. Biomater. Appl. 24 (2009) 293-398.
[16] D. Drago, S. Bolognin, P. Zatta, Role of metal ions in the abeta oligomerization in Alzheimer's disease and in other neurological disorders, Curr. Alzheimer Res. 5 (2008) 500-507.
[17] L.L. Hench, D.E. Clark, Physical chemistry of glass surface, J. Non-Cryst. Solids 28 (1978) 83-105.
[18] L.L. Hench, The story of Bioglass®, J. Mater. Sci. Mater. Med. 17 (2006) 976-978.
[19] H.P. Hood, M.E. Nordberg, Patent US2106744A, 19 march 1934.
[20] N. Kreidl, Phase separation in glasses, J. Non-Cryst. Solids. 129 (1991) 1-11.
[21] H. Arstila, L. Hupa, K.H. Karlsson, M. Hupa, Influence of heat treatment on crystallization of bioactive glasses, J. Non-Cryst. Solids 354 (2008) 722-728.
[22] D. Zhang, M. Hupa, L. Hupa, In situ pH within particle beds of bioactive glasses, Acta Biomater. 4 (2008) 1498-1505.
[23] A. Rafferty, R. Hill, B. Kelleher, T. O'Dwyer, An investigation of amorphous phase separation, leachability and surface area of an ionomer glass system and a sodium-boro-silicate glass system, J. Mater. Sci. 38 (2003) 3891-3902.
[24] B.C. Bunker, Molecular mechanisms for corrosion of silica and silicate glasses, J. Non-Crystal. Solids 179 (1994) 300-308.
[25] A.D. Neve, V. Piddock, E.C. Combe, Development of novel dental cements. I. Formulation of aluminoborate glasses, Clin. Mater. 9 (1992) 7-12.
[26] D. Kim, H.A. Abo-Masallam, H.Y. Lee, G.R. Kim, H.W. Kim, H.H. Lee HH, Development of a novel aluminum-free glass ionomer cement based on magnesium/strontium-silicate glasses, Mater. Sci. Eng. C Mater. Biol. Appl. 42 (2014) 665-671.
[27] F. Gomes, R.A. Pires, R.L. Reis, Aluminum-free glass-ionomer bone cements with enhanced bioactivity and biodegradability, Mater. Sci. Eng. C Mater. Biol. Appl. 33 (2013) 1361-1370.

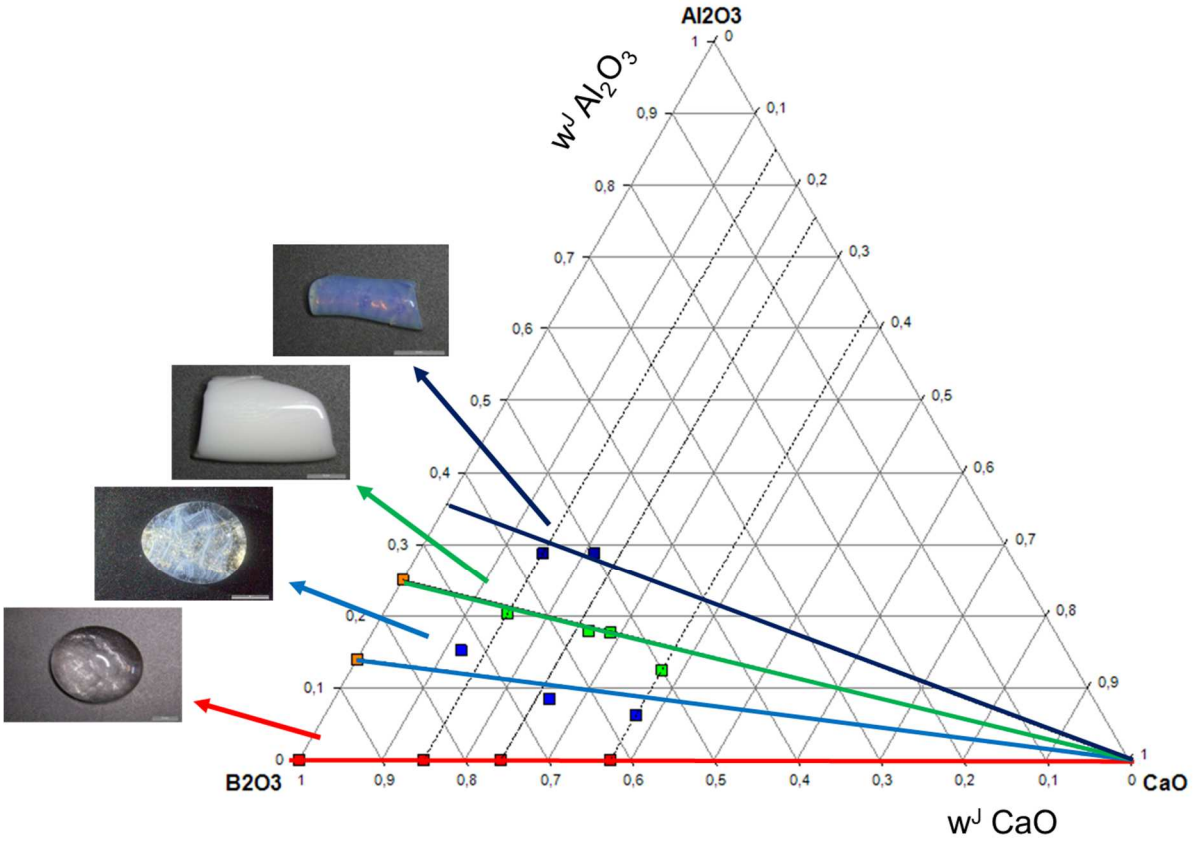

Figure 1. Triaxial diagram showing the relation between the visual aspect and the samples composition in the quinary system SiO_2-B_2O_3-K_2O-Al_2O_3-CaO (composition expressed in Janecke's coordinates, SiO_2 and K_2O being fixed at 45w% and 15w% respectively).

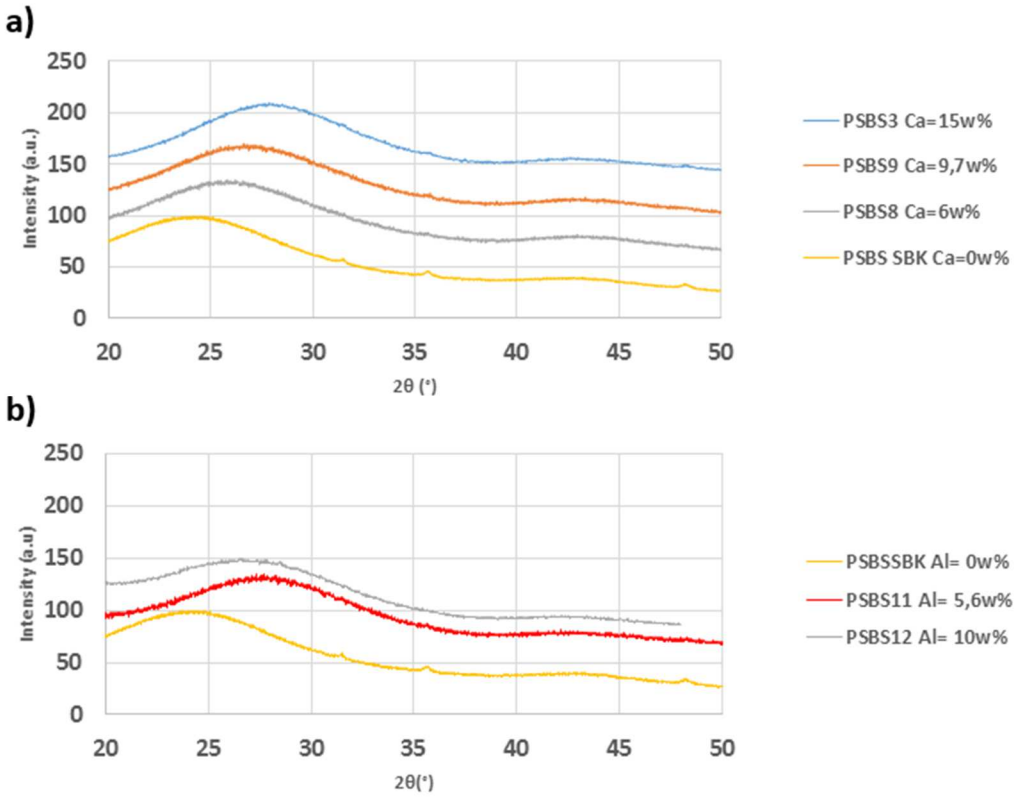

Figure 2. Characteristic amorphous XRD patterns of glasses without Al_2O_3 (a) and without CaO (b).

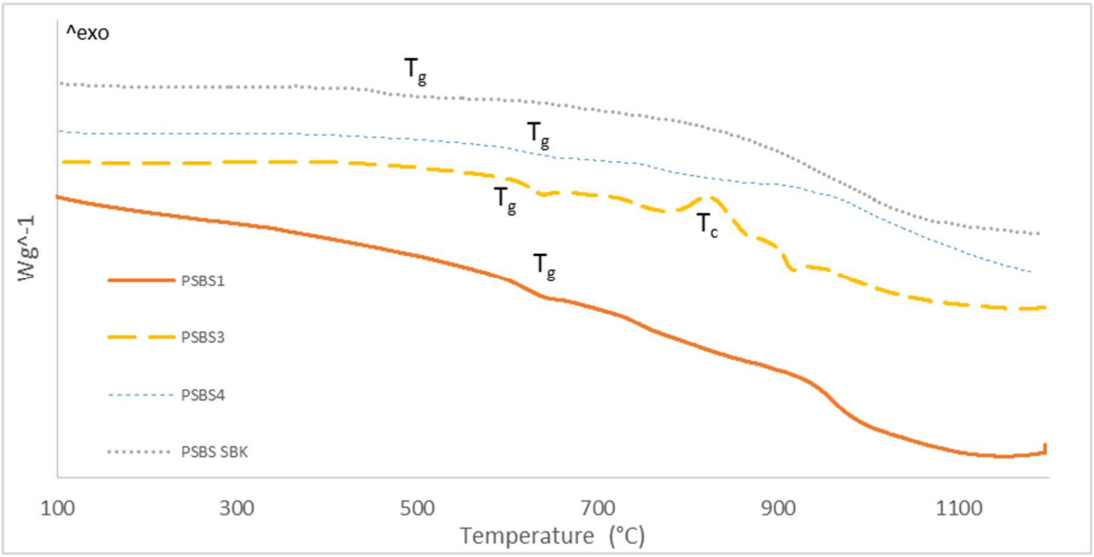

Figure 3. DTA analysis showing the thermal response of PSBS samples with an up scan analysis. The glass transition (Tg) and crystallization phenomenon (Tc above the heat-treatment temperature) are indicated for each curves (relative uncertainty on temperature $u_r(T) = 0.3\%$).

Figure 4. PSBS 3 section showing the development of the crystalline phase after 5h (a), 10h (b) and 20h (c) of 800°C heat-treatment.

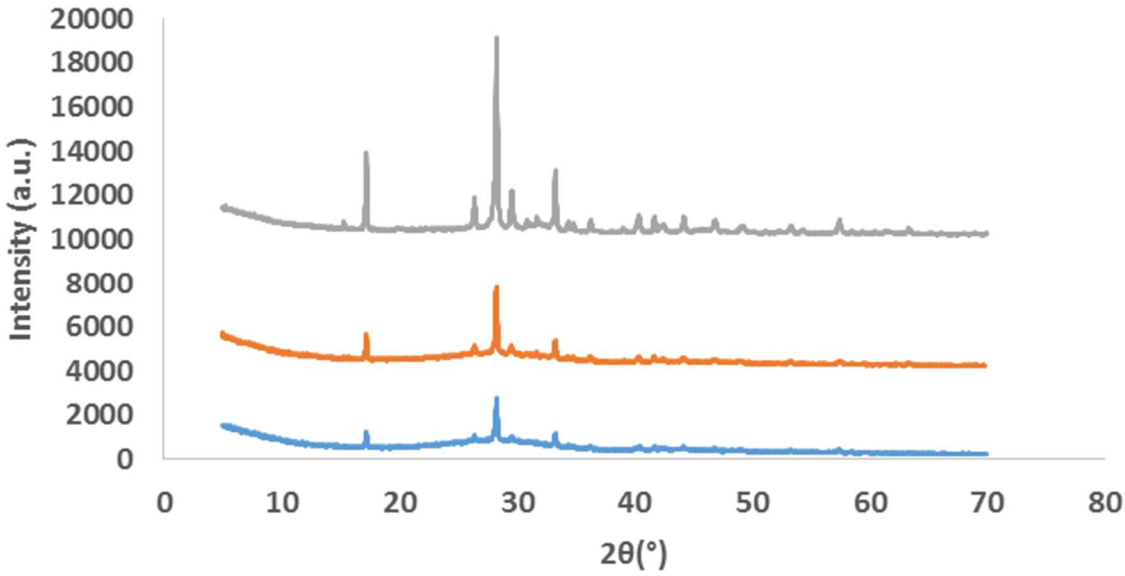

Figure 5. XRD patterns of PSBS 3 heat-treated at 800°C during 5, 10 and 20h.

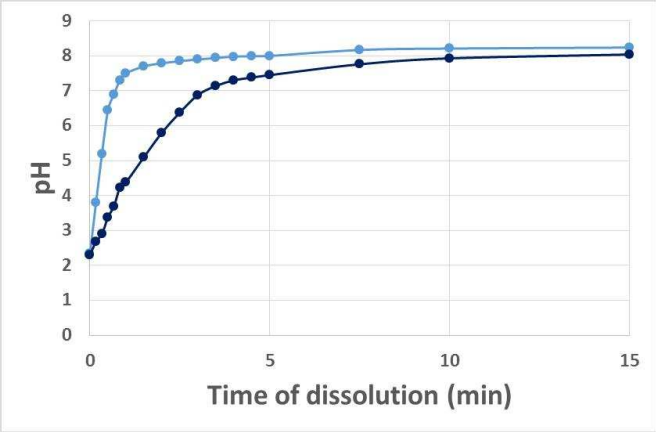

Figure 6. Characteristic pH variation in HNO_3 acid for PSBS before (dark blue line) and after (light blue line) the heat treatment (u(pH) = 0.02)

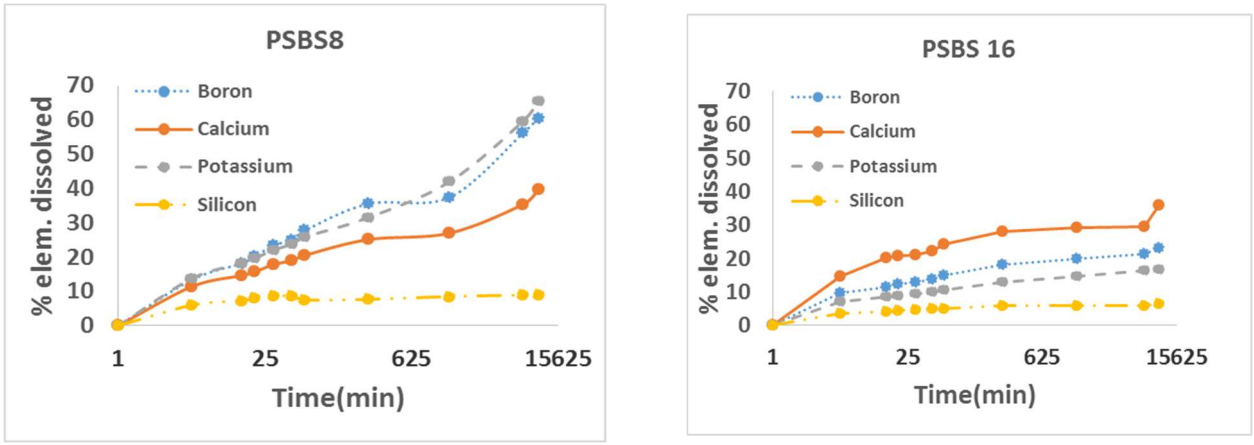

Figure 7. Kinetic study of ion release: comparison between transparent (PBS8) and opalescent (PBS16) glasses. Data are presented on a logarithmic time scale. The releases of boron, calcium, potassium and silicon ions have been detected at different time-points (relative uncertainty on percentage of dissolved element, u_r([element]%) = 3% for Boron, Calcium, Silicon and 5% for Potassium).

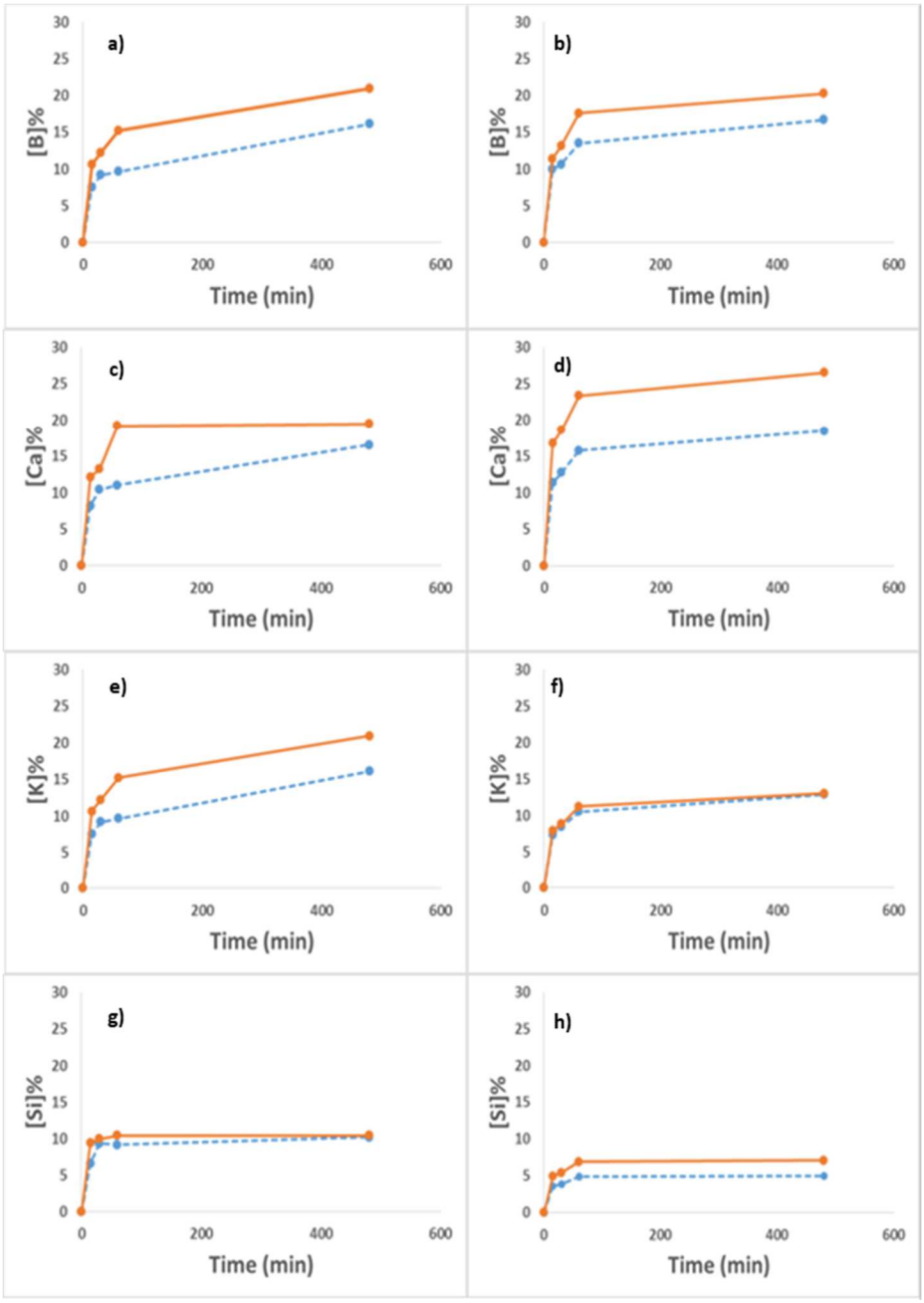

Figure. 8. Comparison of ion release in a transparent PSBS3 (left column graphs) and an opalescent PSBS5 glass sample (right column graphs). The comparison has been made within a heat-treated sample (solid line) and a melt-quenched sample (dotted line) in terms of: the leaching of different ions: boron (a,b), calcium (c,d), potassium (e,f) and silicon (g,h). The y-axis indicates the percentage of the available element in the glass that has dissolved into the acid solution (relative uncertainty on percentage of dissolved element, u_r([element]%) = 3% for Boron, Calcium, Silicon and 5% for Potassium).

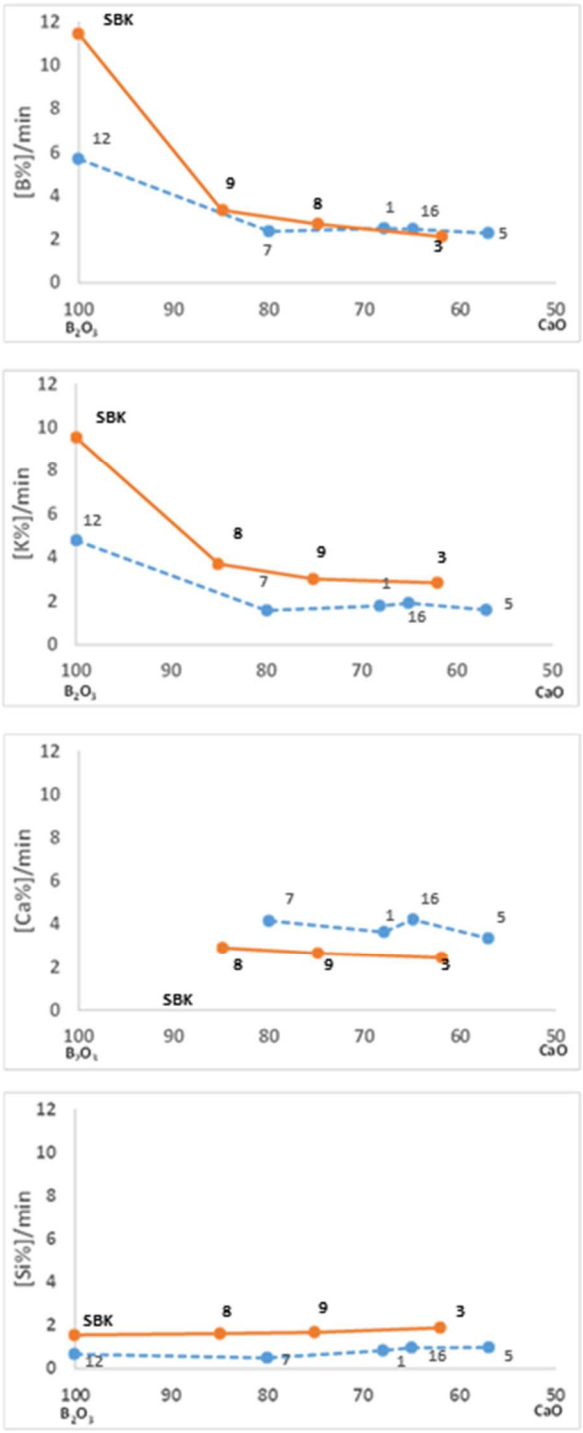

Figure 9. Comparison of ion kinetic release in opalescent (dotted line) and transparent (solid line) glasses. The kinetic release of the ions is calculated as the percentage of the single element dissolved per minute and is related to the B_2O_3/CaO ratio, expressed here as the B_2O_3 and CaO amount in the glasses considering the other elements constant (relative uncertainty on percentage of dissolved element, u_r([element]%) = 3% for Boron, Calcium, Silicon and 5% for Potassium).

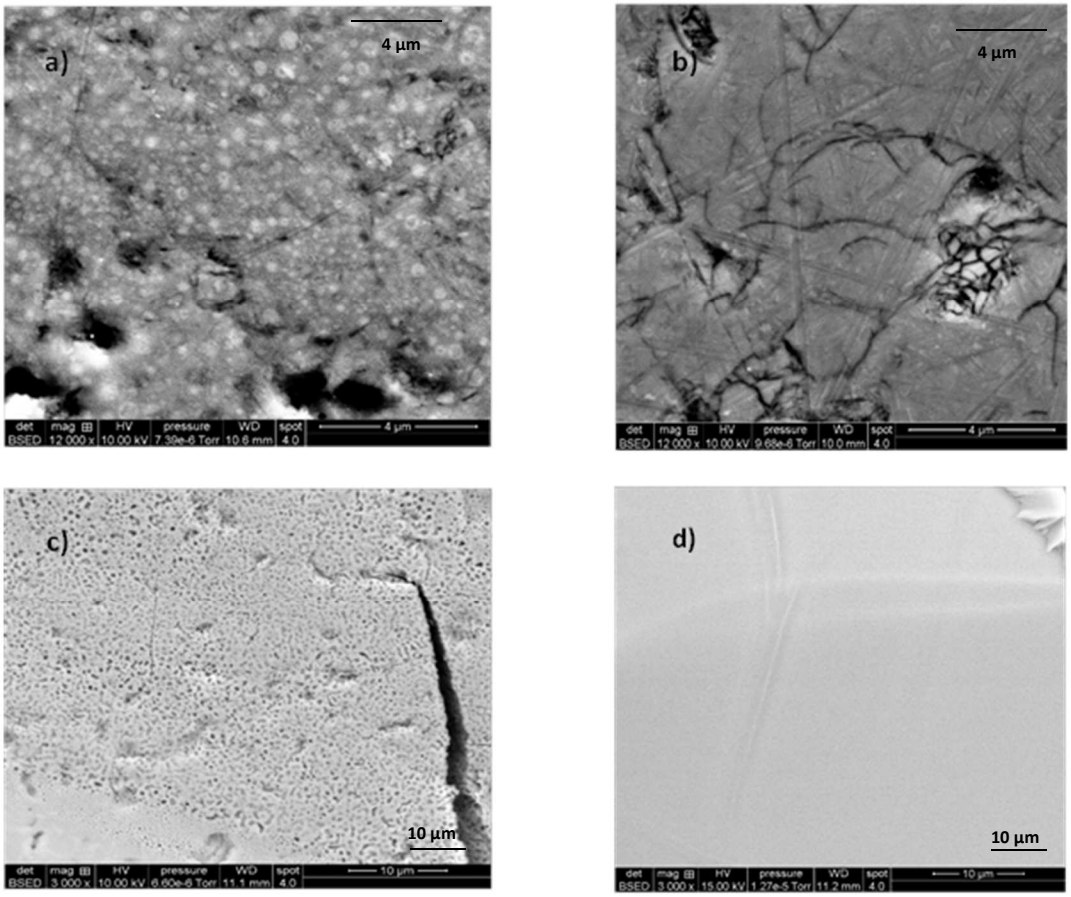

Figure 10. SEM micrographs showing the glass microstructures before (a,b) and after (c,d) the dissolution test in ambient condition (HNO_3 1M aqueous solution, T = 37°C). PSBS16 is presented on the left while PSBS 8 is showed on the right.

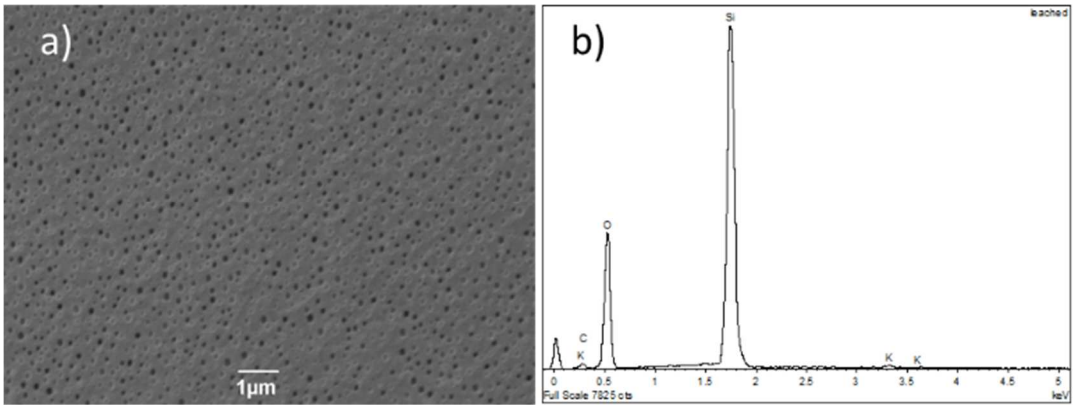

Figure 11. Characterization of retained structures for PSBS 16 after hard condition dissolution experiment (HNO_3 1M aqueous solution, T = 90°C ; a: surface analysis; b: EDX spectrum).

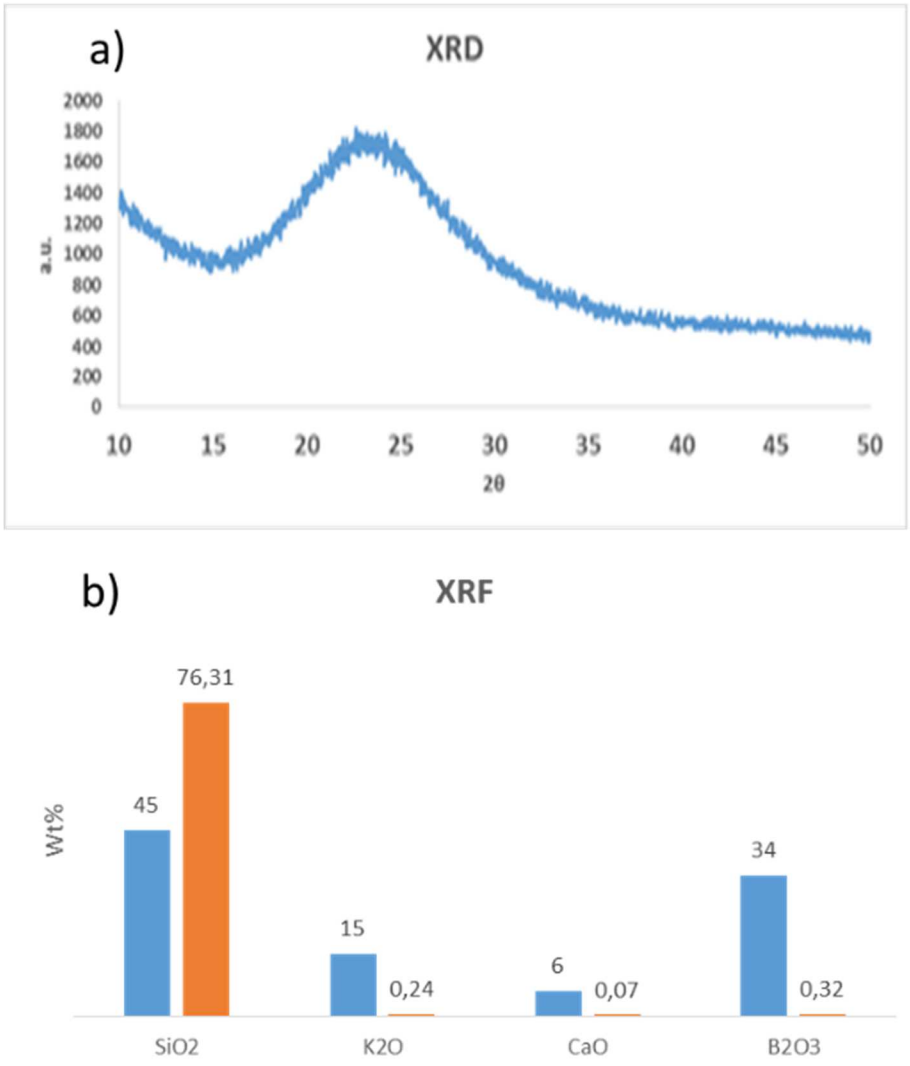

Figure 12. Characterization of the residual glass powder for PSBS 8 after hard condition dissolution experiment (HNO_3 1M aqueous solution, T = 90°C ; a: XRD pattern; b: chemical XRF). The XRF analysis shows the powder after the dissolution (orange column) compared with the initial composition of the glass (blue columns).

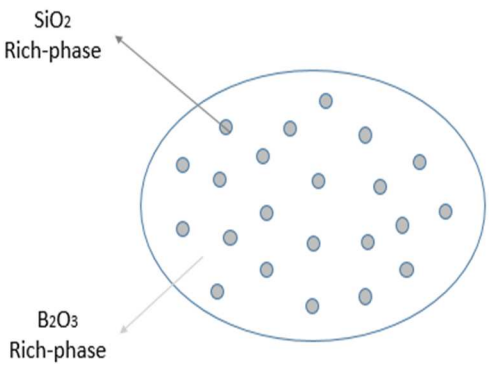

Figure 13. Proposed glass PSBS8 microstructure after the heat treatment: A nucleated structure with a chemically weak continue phase surrounding a droplet phase.

Sample name	B_2O_3	Al_2O_3	CaO
PSBS 1	22.5	7.2	10.4
PSBS 2	26.2	3.4	10.4
PSBS 3	25.0	0.0	15.0
PSBS 4	20.0	11.5	8.5
PSBS 5	20.0	5.0	15.0
PSBS 6	26.2	3.4	10.4
PSBS 7	25.9	8.1	6.0
PSBS 8	34.0	0.0	6.0
PSBS 9	30.3	0.0	9.7
PSBS 10	25.9	8.1	6.0
PSBS 11	34.4	5.6	0.0
PSBS 12	30.0	10.0	0.0
PSBS 13	22.5	11.5	6.0
PSBS 14	22.5	2.5	15.0
PSBS 15	29.1	4.8	6.1
PSBS 16	21.4	7.1	11.5
PSBS SBK	40.0	0.0	0.0

Table 1. Composition of the experimental borosilicate glasses (composition expressed in w%, SiO_2 and K_2O being fixed at 45w% and 15w% respectively).

Element	Emission lines
B	208.956, 249.678, 249.772 nm
Ca	317.993, 373.690 nm
K	766.49, 769.897 nm
Si	250.690, 251.611, 288.158 nm

Table 2. Elements detected with ICP measurements and respective emission lines.

Sample	PSBS SBK	PSBS 8	PSBS 9	PSBS 3	PSBS 11	PSBS 12
2θ angle (degree)	24.55	25.80	26.64	27.83	26.80	26.06
d-spacing (Å)	3.69	3.41	3.29	3.19	3.53	3.45
CaO (w%)	0.0	6.0	9.7	15.0	0.0	0.0
Al_2O_3 (w%)	0.0	0.0	0.0	0.0	5.6	10.0

Table 3. Evolution of the diffraction parameters in relation with the calcium content (w%) in different Al-free PSBS glass samples.

Sample	PSBS SBK	PSBS 1	PSBS 3	PSBS 4
Al_2O_3 (w%)	0	7.2	0	11.5
CaO (w%)	0	10.4	15	8.5
HT Tg (°C)	438.9	598.1	610.7	589.6
Tc (°C)	n/o	n/o	787.8	n/o

Table 4. Glass transition temperature of the heat-treated glasses (HT) compared with the Al_2O_3 and CaO content in the sample (relative uncertainty on temperature $u_r(T) = 0.3\%$).